frontiers | Frontiers in Materials

TYPE Original Research
PUBLISHED 28 September 2022
DOI 10.3389/fmats.2022.1015322

Structural damage detection based on modal feature extraction and multi-objective optimization method for steel structures

Zepeng Chen[1,2]*, Di Zhao[1], Zhou Chen[1] and Wenxue Wang[3]

[1]School of Transportation and Civil Engineering and Architecture, Foshan University, Foshan, China, [2]MOE Key Lab of Disaster Forecast and Control in Engineering, Jinan University, Guangzhou, China, [3]Research Institute for Applied Mechanics, Kyushu University, Fukuoka, Japan

OPEN ACCESS

EDITED BY
Zhicheng Yang,
Zhongkai University of Agriculture and Engineering, China

REVIEWED BY
Yizhou Lin,
Dongguan University of Technology, China
Jie Wu,
Wuhan Polytechnic University, China

*CORRESPONDENCE
Zepeng Chen,
zpchen2014@foxmail.com

SPECIALTY SECTION
This article was submitted to Structural Materials,
a section of the journal
Frontiers in Materials

RECEIVED 09 August 2022
ACCEPTED 29 August 2022
PUBLISHED 28 September 2022

CITATION
Chen Z, Zhao D, Chen Z and Wang W (2022), Structural damage detection based on modal feature extraction and multi-objective optimization method for steel structures.
Front. Mater. 9:1015322.
doi: 10.3389/fmats.2022.1015322

Model updating based on intelligent algorithms has achieved great success in structural damage detection (SDD). But the appropriate selection of objective functions remains unclear and becomes an obstacle to applying the methods to real-world steel structures. In this paper, a multi-objective identification method based on modal feature extraction and linear weight sum was proposed, and the best weight values to gain the best solution were also determined. A hybrid particle swarm optimization (HPSO) was selected as a solver to update structural parameters for accurate SDD results. First of all, six single objective functions based on modal feature extraction were considered, and numerical simulations show that the one based on MTMAC indicator exhibits certain superiority over the other. In order to provide a fair comparison among different objective functions, a quantified indicator named damage vector consistency (DVC) is also defined, which describes the consistency between identified result and the assumed one. After that, a multi-objective identification method is formulated by linearly combining an MTMAC-based objective function and another selected single objective function. Different weight values were also investigated to find out the best solution for accurate SDD. Three numerical simulations were conducted, including a simply-supported beam, a two-story steel frame, and a 31-bar plane truss. Their SDD results verify the applicability of the proposed multi-objective optimization method. Some relative discussions are also described in detail.

KEYWORDS

structural damage detection (SDD), modal feature extraction, multi-objective optimization, damage vector consistency, steel structures

Introduction

During the past decades, structural health monitoring (SHM) has received rapidly increasing attention because it can help to protect structures from severe damage (Hou and Xia, 2021). An integral SHM system contains a lot of different kinds of sensors that should be installed on structures to record various types of responses (Yi et al., 2015, 2017; Xiong et al., 2021). Nowadays civil structures such as Guangzhou New TV Tower, Tsing Ma Bridge, and Hong Kong-Zhuhai-Macao Bridge are equipped with advanced SHM systems to ensure the serving structures are in healthy condition (Miguel et al., 2009; He et al., 2022). Structural damage detection (SDD) is an important issue in the SHM field, and it is the ultimate goal of SHM. There have been lots of SDD methodologies proposed to extract damage-sensitive features from the recorded responses and identify structural damage ultimately.

A comparison between two different structural states is required for SDD results (Worden et al., 2007). But actually, it is hardly possible to discover anomalies directly from the measured responses. Therefore, some damage-sensitive features should be previously extracted to obviously show changes due to damage (Lin et al., 2017). The application of damage-sensitive features for SDD can be divided into two categories: model-free and model-based identification methods.

The model-free identification methods aim to detect variation in damage-sensitive features and then identify damages based on the variation. Modal feature extraction has been widely used to generate damage-sensitive indicators. Changes in natural frequencies (Cawley and Adams, 1979) were verified effective to be effective in detecting damage in two-dimension structures. However, it possibly becomes invalid because two scenarios with symmetrical damages in a symmetrical structure would give the same changes in natural frequencies. So, indicators based on mode shapes emerged, which are more sensitive to damage location (West, 1986). After that, more indicators based on the derivation of mode shapes and natural frequencies, such as mode shape curvatures (Pandey et al., 1991), modal flexibility (Pandey and Biswas, 1994), and modal strain energy (Shi et al., 1998; Zhang et al., 2022), were subsequently presented for better SDD results. Moreover, damage-sensitive features extracted from recorded responses based on statistical methods or special transformations have also been developed. The principal component analysis is a typical statistical technique, and the error between the reconstructed response, a combination of the first few principal components, and the original one is verified available to recognize the onset of damage (Boe and Golinval, 2003; Yan et al., 2005). Methodologies based on higher statistical moments show their capability to distinguish nonlinear damage from responses affected by environmental and operational conditions (Yu and Zhu, 2015, 2017). Furthermore, methods of time series analysis model are also feasible in model-free identification (Yu and Zhu, 2015; Yu and Lin, 2017). Besides, the variation of translated coefficients according to signal processing methods, such as wavelet transformation (Hou et al., 2000), wavelet package transform (Law et al., 2005), Hilbert-Huang transformation (Yang et al., 2004), and empirical mode decomposition (Xu and Chen, 2004), have also been introduced to SDD. Recently, a widespread interest in feature extraction based on Bayesian inference has also been developed (Mu and Yuen, 2017). However, the model-free identification method is usually only used to determine the occurrence of damage because it can hardly quantify or locate structural damage. On the contrary, the model-based identification method can effectively identify damages' extent and location so that it becomes more and more popular in SDD.

The model-based identification method aims at minimizing the discrepancy of damage-sensitive features between the target structure and the numerical one so that the latter can serve as a surrogate to reflect structural health condition. In this way, the SDD problem is usually simplified as an optimal problem mathematically, and the corresponding approach is named model updating. A typical model updating contains three major parts: damage-sensitive features extraction, optimization algorithm selection, and objective function definition. The first part is the same as that mentioned in the above paragraph. In the second part, a proper optimization algorithm should be selected to do repeated iterations until an accurate SDD result is gained. There are now three major types of optimization algorithms: sensitivity analysis, intelligent algorithm, and Bayesian theory. The sensitivity analysis usually involves the ill-conditioned problem because of the sensitivity matrix's singularity and noise involvement (Jaishi and Ren, 2006). It leads to inaccurate and unstable SDD results. To improve the method, various types of regularization methods, such as Tikhonov regularization (Lu et al., 2017), truncated singular value decomposition (Chen, 2008) and sparse regularization (Hou et al., 2018), have been introduced. Bayesian theory is firstly presented by James (Beck et al., 2001). Parameters and responses in this method are all considered uncertain, which is verified effective in dealing with SDD problems involving uncertainty, such as model error, noise contamination and uncertain supports (Lu et al., 2020, 2021). The SDD results based on Bayesian model updating are probabilistic, and it is a significant difference compared with those determined model updating such as sensitivity analysis. A great challenge in Bayesian model updating is the calculation of marginal probabilities, which involves high-dimension integration (Cheung and Beck, 2009). Methods such as Metropolis-Hastings algorithm (Beck and Au, 2002), transitional Markov chain Monte Carlo method (Ching and Chen, 2007), hybrid Monte Carlo simulation (Cheung and Beck, 2009) and so on, have made improvement. Moreover, robust Bayesian compressive (Huang et al., 2014), hierarchical Bayesian model updating (Behmanesh et al., 2015), sparse Bayesian learning (Hou et al., 2019) and Robust sparse

Bayesian learning (Wang et al., 2022) have been developed to improve the SDD efficiency as well. However, the complicated determination of marginal probabilities and low calculation efficiency remains challenge and restrict the method's application in complex structures. Finally, the intelligent algorithm has been popularly applied to SDD because of its simplicity and outstanding performance in use. The intelligent algorithm is a trial-and-error algorithm. Different kinds of intelligent algorithms (Yu and Li, 2014; Chu-Dong et al., 2016; Chen and Yu, 2018; Ding et al., 2019a, 2022; Chen et al., 2019; Minh et al., 2022) have been proposed and achieved successful application in SDD. The basic procedures of an intelligent algorithm include candidate generation, candidate updating, and stop criterion. However, stable and efficient optimal strategies are significant to improve the algorithms. The first commonly used strategy introduces new updating strategies into the original algorithm in order to make it much more capable for specific SDD cases (Rao et al., 2004; Liu et al., 2005; Ding et al., 2018). The second one is to formulate a hybrid algorithm combined with two or more different algorithms so that each can show its advantages (He and Hwang, 2006; Baghmisheh et al., 2012; Ding et al., 2019b). The final one is a multi-step algorithm that different algorithms are applied to different SDD levels in order to accelerate the solving process with satisfactory accuracy (Perera and Ruiz, 2008; Seyedpoor, 2012). In this paper, a hybrid algorithm proposed by Chen and Yu (2018) is utilized to deal with SDD.

As the critical component, the objective function definition is essential in connecting the damage-sensitive features and the optimization algorithms. The objective function is essentially a calculation of distance. It measures the difference between the numerical model and the target one by determining the discrepancy of the damage-sensitive features. And SDD results will be gained if the discrepancy is minimized. The single objective function is commonly used in SDD. Modal parameters, such as frequencies and mode shapes, have been widely applied to define objective functions based on Euler distance or cosine distance (Chen and Yu, 2018; Chen et al., 2019). Furthermore, modal assurance criterion (MAC), coordinate modal assurance criteria (COMAC) (Lieven and Ewins, 1988), multiple damage location assurance criterion (MDLAC) (Messina et al., 1998), total modal assurance criterion (TMAC) (Gao and Spencer, 2002), modified total modal assurance criterion (MTMAC) (Perera and Torres, 2006) and so on have been successfully applied for objective function definition and showed good performance in SDD. However, the single objective functions sometimes converge to an incorrect solution because the noise-contaminated response brings errors in the extracted features. A feasible solution to deal with this problem is using multi-objective optimizations (Jung et al., 2010). On the one hand, feasible solutions based on multi-objective optimization are less than that based on single-objective optimization. On the other hand, the Pareto-optimal solutions provide a higher possibility of capturing the true solution. Perera et al (2007) investigated the multi-objective optimization based on niched Pareto genetic algorithm (NPGA), and their SDD results showed the feasible application of modal flexibility in multi-objective optimization. After that, they also firstly compared capability of several evolutionary techniques utilizing multi-objective optimization (Perera et al., 2009). Furthermore, the combination of dynamic and static measurements in multi-objective function definition also showed enhancement of prediction in SDD (Perera et al., 2013). In the work of Cha and Buyukozturk (2015), they proposed a hybrid multi-objective optimization based on modal strain energy and successfully applied the method for detecting minor damages in three-dimensional (3-D) steel structures. However, the appropriate selection of objective function still remains unclear in SDD and becomes an obstacle for the application of the methods to real-world steel structures.

In this paper, a multi-objective identification method based on modal data and linear weight sum was proposed. First, a comparison of SDD results among six single objective functions based on modal feature extraction was conducted, and the most accurate one was determined for multi-objective function definition. Then, the best weight values to combine two different objective functions into an excellent multi-objective function was also determined. In this way, the most suitable objective function for SDD of steel structures can be obtained and it also provides guidance in selecting a proper objective function. A HPSO is selected to solve SDD problems, and a quantified indicator named damage vector consistency (DVC) is also defined to make a fair comparison among different SDD methods. Numerical simulations, including a simply-supported beam, a two-story steel frame, and a 31-bar plane truss with several assumed damage cases, are performed to verify the proposed methods' effectiveness.

This paper is organized as follows. Section one is devoted to the literature review, containing an introduction of the SDD problem and a detailed description of model updating in SDD. The basic theory of SDD is briefly described in section two. A detailed description of the proposed multi-objective optimization method and the proposed quantified indicator are also presented in this section. Numerical simulation of a simply-supported beam is presented in section three, and some factors, such as weight values and noises, are also discussed based on the beam model. In section four, two two-dimensional structures, including a frame and a truss, are further investigated to show the method's applicability in different structures. Finally, some conclusions are drawn and discussed in section five.

Theoretical background

Basic theory of model updating

Based on the finite element (FE) model theory, the analytical structure is divided into several elements with specific material and physical parameters. And SDD tries to figure out the changes in the elemental parameters. Several methods have been proposed to describe structural damage; among them, the reduced stiffness method is widely used because of its simplicity and specific physical meaning. In the method, a damage factor vector $\boldsymbol{\alpha}$ is introduced in a prior, and then the damaging effect on structural stiffness $\mathbf{K}$ can be therefore described as a linear combination of element stiffness matrix, which is mathematically shown as follows,

$$\mathbf{K}(\boldsymbol{\alpha}) = \sum_{i=1}^{N_{ele}} (1-\alpha_i)\mathbf{K}_i \tag{1}$$

where N_{ele} is the number of elements. And α_i, the damage factor component at the ith element, ranges from 0 to 1. Especially, $\alpha_i = 0$ means the ith element is healthy. $\mathbf{K}_i$ represents the ith element stiffness matrix. Combining with the reduced stiffness method, the model updating is formulated as follows,

$$\boldsymbol{\alpha}_{opt} = \arg\min_{\boldsymbol{\alpha}} J(\boldsymbol{\alpha}) \tag{2}$$

in which $\boldsymbol{\alpha}_{opt}$ is the optimal damage factor vector, and $J(\boldsymbol{\alpha})$ is the objective function.

Hybrid particle swarm optimization (HPSO)

PSO is an intelligent algorithm and also a population-based and self-adaptive search technique. Kennedy and Eberhart (1995) formulated the original PSO mathematically. It has shown well-performance in SDD. The updating process of PSO is formulated as below,

$$\begin{aligned} v_i^{k+1} &= w\cdot v_i^k + c_1\cdot r_1\cdot\left(x_{ib}^k - x_i^k\right) + c_2\cdot r_2\cdot\left(x_g^k - x_i^k\right)\\ x_i^{k+1} &= x_i^k + v_i^{k+1}\\ x_{ib}^{k+1} &= \begin{cases} x_i^{k+1}, J\left(x_i^{k+1}\right) < J\left(x_{ib}^k\right)\\ x_{ib}^k, otherwise\end{cases}, x_g^k = \begin{cases} x_g^{k+1}, J\left(x_g^{k+1}\right) < J\left(x_g^k\right)\\ x_g^k, otherwise\end{cases}\end{aligned} \tag{3}$$

in which the subscript i and the superscript k mean the ith particle and the kth iteration, respectively; v and x are the velocity and position of the particle, respectively. W is an inertia weight; r_1 and r_2 are two uniformly distributed numbers ranging from 0 to 1; c_1, c_2 are learning factors named cognitive and social coefficients, respectively; x_{ib} is the best-known position of individual particle and x_g is the best-known position of the entire swarm. $J(\boldsymbol{\alpha})$ is the objective function.

The PSO randomly select a specific number of candidate solutions from the feasible region and then updates them based on Eq. 3 until the stop criterion is met. However, the original PSO easily converges to a local minimum in some SDD cases. HPSO is one of the improving methods combining the PSO and improved Nelder-Mead optimization. The effectiveness and efficiency of HSPO both in numerical simulations and experimental tests have been verified in the paper of Chen and Yu (2018). Therefore, the HSPO is selected as the optimization method in this paper.

Multi-objective identification method

In the multi-objective identification method, the SDD is achieved by minimizing more than one single objective function simultaneously. So, the multi-objective function is mathematically formulated as,

$$J(\boldsymbol{\alpha}) = [J_1(\boldsymbol{\alpha}), J_2(\boldsymbol{\alpha}), \ldots, J_3(\boldsymbol{\alpha})] \tag{4}$$

The solution to the multi-objective optimization problem is more than one because a single point cannot be an optimum for all the objectives. Instead, a set of alternative solutions will be gained, and the best one should be selected from them. There are different methods to solve multi-objective damage identification problems, such as linear weighting sum method, weighted min-max method, niched-Pareto genetic algorithm, strength Pareto evolutionary algorithm, and so on. This paper considers only two single objective functions because more than three objectives will be computationally too expensive.

The linear weighting sum method (LWS) is applied to the proposed method. Based on LWS, a single objective is formulated based on the linear combination of two objectives, and two weighting factors, w and (1-w), are therefore introduced. The aggregating function is formulated as,

$$J(\boldsymbol{\alpha}) = wJ_1(\boldsymbol{\alpha}) + (1-w)J_2(\boldsymbol{\alpha}) \tag{5}$$

The selection of weights creates a balance between different objectives, and their relative value also shows the relative importance of the objectives. However, the choice of weights is arbitrary because the importance of each objective is unknown in advance. By varying the weights, a set of Pareto-optimal solutions is obtained. After that, the Pareto-optimal solutions are compared with each other based on damage vector consistency (DVC) which will be described below.

Six single objective functions based on modal feature extraction are selected in this paper. The first one is based on frequency change rate (FCR), which is shown as,

$$SObj_1(\boldsymbol{\alpha}) = \sum_{i=1}^{n_M} FCR(f_i, f_i(\boldsymbol{\alpha})) = \sum_{i=1}^{n_M}\left|\frac{f_i^m - f_i(\boldsymbol{\alpha})}{f_i^m + f_i(\boldsymbol{\alpha})}\right| \tag{6}$$

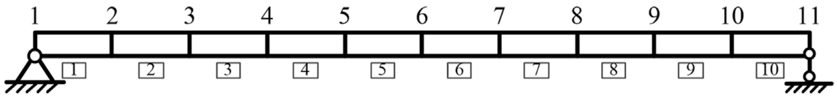

FIGURE 1
Finite element model of simply-supported beam.

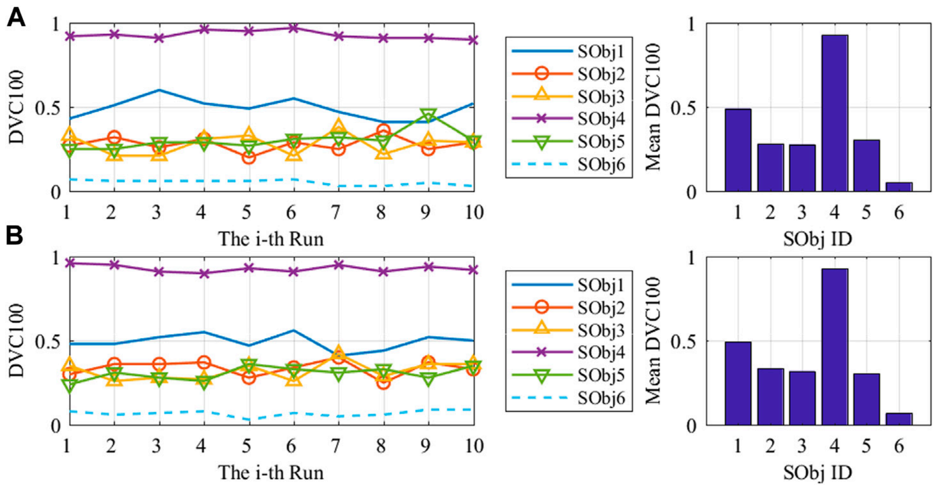

FIGURE 2
SDD results in case 1 **(A)** N_M = 3. **(B)** N_M = 5.

in which f_i and $f_i(\alpha)$ are the *ith* targeted and the *ith* calculated frequency, respectively. n_M is the selected number of modes. The second one is formulated by the MAC shown as,

$$SObj_2(\boldsymbol{\alpha}) = \sum_{i=1}^{n_M}\left[1 - MAC(\varphi_i, \varphi_i(\boldsymbol{\alpha}))\right] = \sum_{i=1}^{n_M}\left[1 - \frac{(\varphi_i^T\varphi_i(\boldsymbol{\alpha}))^2}{(\varphi_i^T\varphi_i)\varphi_i^T(\boldsymbol{\alpha})\varphi_i(\boldsymbol{\alpha})}\right] \tag{7}$$

in which φ_i and $\varphi_i(\alpha)$ are the *ith* targeted and the *ith* calculated modal shape, respectively. The third one is defined based on the TMAC, and its mathematical expression is shown as,

$$SObj_3(\boldsymbol{\alpha}) = 1 - TMAC = 1 - \prod_{i=1}^{n_M} MAC(\varphi_i, \varphi_i(\boldsymbol{\alpha})) \tag{8}$$

As seen above, only the frequency or the modal shape is considered in an objective. In order to improve the application of the objectives in different kinds of damage cases, both frequencies and mode shapes should be further contained. Therefore, the TMAC can be improved by introducing the frequency, and the fourth single objective function is subsequently formulated as,

$$SObj_4(\boldsymbol{\alpha}) = 1 - MTMAC = 1 - \prod_{i=1}^{n_M}\frac{MAC(\varphi_i, \varphi_i(\boldsymbol{\alpha}))}{\left(1 + \left|\frac{f_i - f_i(\boldsymbol{\alpha})}{f_i + f_i(\boldsymbol{\alpha})}\right|\right)} \tag{9}$$

in which $\left|\frac{f_i - f_i(\boldsymbol{\alpha})}{f_i + f_i(\boldsymbol{\alpha})}\right|$ is regarded as a penalty function due to the differences between targeted and calculated frequencies. The MTMAC varies from 0 to 1, and MTMAC equaling to 1 means the corresponding $\boldsymbol{\alpha}$ is the same as the assumed one. Furthermore, the modal flexibility defined by frequencies and mode shapes is also selected as a damage indicator and therefore formulates the fifth objective function shown as,

$$SObj_5(\boldsymbol{\alpha}) = 1 - MACFLEX = 1 - \prod_{i=1}^{n_M}\frac{(F_i^T F_i(\boldsymbol{\alpha}))^2}{(F_i^T F_i)F_i^T(\boldsymbol{\alpha})F_i(\boldsymbol{\alpha})} \tag{10}$$

in which F_i and $F_i(\boldsymbol{\alpha})$ represent the *ith* targeted and the *ith* calculated modal flexibility, respectively. And $F_i = (\varphi_i\ \varphi_i^T)/f_i^2$.

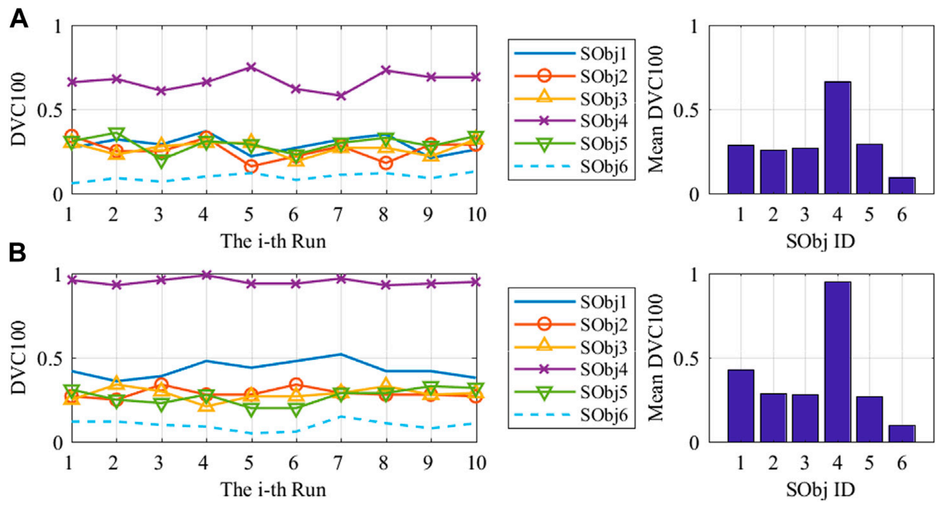

FIGURE 3
SDD results in case 2 **(A)** N_M = 3. **(B)** N_M = 5.

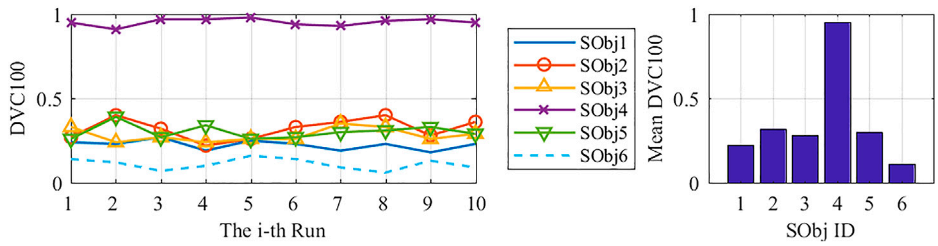

FIGURE 4
SDD results in case 3 using the first five modes.

TABLE 1 DVC100 values of SDD results in case 3 based on *w* = 0.5.

$J_1(\alpha)$	$J_2(\alpha)$	case 2		case 3	
		3 modes	5 modes	3 modes	5 modes
SObj4	*SObj1*	32%	85%	20%	71%
SObj4	*SObj2*	4%	44%	29%	84%
SObj4	*SObj3*	7%	40%	44%	96%
SObj4	*SObj5*	11%	52%	31%	87%
SObj4	*SObj6*	60%	93%	97%	84%

Indicator defined by the MDLAC measures the differences in mode shapes between the undamaged and damaged structure. It not only can well predict damage location but also determine damage extent. Therefore, the final objective function is defined by MDLAC, and it is shown as,

$$SObj_6(\boldsymbol{\alpha}) = \sum_{i=1}^{n_M} \left[1 - MDLAC\left(\Delta\varphi_i, \Delta\varphi_i(\boldsymbol{\alpha})\right)\right] = \sum_{i=1}^{n_M} \left[1 - \frac{\left(\Delta\varphi_i^T \Delta\varphi_i(\boldsymbol{\alpha})\right)^2}{\left(\Delta\varphi_i^T \Delta\varphi_i\right)\Delta\varphi_i^T(\boldsymbol{\alpha})\Delta\varphi_i(\boldsymbol{\alpha})}\right] \tag{11}$$

TABLE 2 DVC100 values of SDD results in case 3 based on varying w and N_M = 5.

$J_1(\alpha)$	$J_2(\alpha)$	N_M	w										
			0	0.1	0.2	0.3	0.4	0.5	0.6	0.7	0.8	0.9	1.0
SObj4	SObj1	5	22%	57%	59%	57%	66%	71%	78%	78%	78%	78%	95%
SObj4	SObj2	5	32%	94%	92%	90%	91%	88%	87%	87%	84%	79%	95%
SObj4	SObj3	5	28%	100%	99%	98%	97%	96%	92%	90%	83%	78%	95%
SObj4	SObj5	5	30%	97%	97%	96%	94%	87%	92%	90%	91%	86%	95%
SObj4	SObj6	5	11%	79%	83%	83%	83%	84%	90%	92%	94%	96%	95%

in which $\Delta\varphi_i$ equals that φ_i minus $\varphi_i(\boldsymbol{\alpha})$.

Damage vector consistency (DVC)

In order to provide a quantificational description of identification accuracy, the DVC is presented describing the consistency between the optimal and the assumed damage factor vector, represented by $\boldsymbol{\alpha}_{opt}$ and $\boldsymbol{\alpha}_{ass}$ respectively. The formulization of the DVC is shown as.

$$DVC = \frac{\left|\alpha_{opt}^T \times \alpha_{ass}\right|}{\left|\alpha_{opt}\right|_2 \times \left|\alpha_{ass}\right|_2} \times 100\% \tag{12}$$

When a vector is closely equaled to another one, the value of DVC approximately equals to 100%. It means the SDD result is accurate and the corresponding method has great ability in dealing with SDD.

Intelligent algorithms sometimes converge to a local optimal in a single calculation. In order to obtain a stable SDD result, an identification run of one damage case usually contains several times of calculations. So, DVC100, the percentage of DVC equaling to 100% in a run, is defined to show how stable SDD results are in repeated calculations. And its value is equaled to,

$$DVC100 = \frac{N_{acu}}{N_{run}} \tag{13}$$

in which, N_{acu} and N_{run} mean the number of calculation times with DVC equaling to 100% and the total calculation times in a run, respectively.

Numerical verifications of simply-supported steel beam

As shown in Figure 1, a simply-supported beam structure model is considered. The beam has the length of 3 m and is divided into 10 elements equally. The material parameters are simulated as Young's modulus 210 GPa and density 7,850 kg/m^3. The area and the moment of inertia of the cross-section are A = 1.164e-3 m^2 and I = 7.6165e-7 m^4, respectively. The first five frequencies of the structure are 23.0917, 92.3762, 207.9352, 370.0772, and 579.5677 Hz.

Three different kinds of damage cases, including single and multiple damages, are assumed. Three assumed cases are shown as, case 1: 20%@5; case 2: 20%@3, 20%@5; case 3: 20%@3, 40%@5, 20%@10; The symbol 20%@5 indicates that the stiffness reduction of the 5th element is 20%, similar meaning for other cases. The SDD based on intelligent algorithms sometimes converges to a local optimal in a single calculation. In this paper, 100 times of calculations based on HPSO is regarded as a run of SDD, and 10 runs are conducted to show the SDD results of different damage cases.

Comparison of SDD results based on single objectives

In this section, the first three and five modes are considered in the objectives definition to show the effect of N_M on SDD accuracy. The SDD results of case 1, utilizing the six different single objectives, are shown in Figure 2. The fluctuation of the DVC100 values due to a specific objective function is small, which means DVC100 is an effective index to quantify the accuracy of the SDD methods. Besides, DVC100 values show a noticeable difference if the objective functions differ. Among all

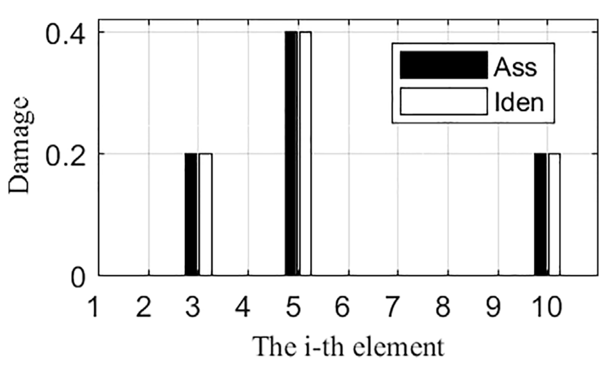

FIGURE 5
Mean values of SDD results in case 3 based on (0.1**SObj*4 + 0.9**SObj*3).

TABLE 3 DVC100 values of SDD results in case 3 based on w = 0.5.

$J_1(\alpha)$	$J_2(\alpha)$	Case 3	
		N_M=3	N_M=5
$SObj1$	$SObj2$	29%	84%
$SObj1$	$SObj3$	28%	89%
$SObj1$	$SObj4$	20%	71%
$SObj1$	$SObj5$	87%	96%
$SObj1$	$SObj6$	84%	80%

the selected single objectives, the $SObj4$ defined based on MTMAC has the highest DVC100 value even if only the first three modes are considered, and the $SObj1$ based on FCR comes second. However, the other objectives have poor DVC100 values, which means the accuracy of their SDD results is far from enough. Also, it can be found that the value of N_M has only a slight effect on SDD accuracy of the single damage cases because their mean DVC100 values are almost the same.

However, the SDD results shown in Figure 3 of case 2 show a little difference. A significant decline occurs in DVC100 when only the first three modes are considered. It means the SDD results based on the first three modes are less accurate than those based on the first five. This is different from that in the single damage case, indicating that more modes should be required for accurate SDD in multi-damage cases. On the other hand, no matter how many modes are considered, the $SObj4$ defined based on MTMAC exhibits certain superiority over the other objectives as its DVC100 values are all greater than others.

Therefore, the first five modes are considered in case 3, and the SDD results are shown in Figure 4. The results also provide strong evidence that the $SObj4$ performs better than the other objectives.

Verifications of the proposed method

Based on the above section, the best single objective among the selected six is $SObj4$. Therefore, $SObj4$ is selected as $J_1(\alpha)$ as shown in Eq. 5, and the other five single objectives are regarded as $J_2(\alpha)$ alternatively. Firstly, the weight value of $J_1(\alpha)$ is set to be 0.5, which means equal importance for both objectives. Then, the DVC100 values of SDD results for cases 2 and 3 are listed in Table 1, which are calculated based on the 100 times of calculation results. It can be seen that the DVC100 values only considered the first three modes are pretty low. Moreover, it also means more than three modes should be considered even in multi-objective optimization. However, once the first five modes are considered, the DVC100 values significantly increase. Under the conditions of w = 0.5 and N_M = 5, the multi-objective function combining $SObj4$ and $SObj6$ is the best because DVC100 values based on it keep a high value in both cases. However, the summation of $SObj4$ and another single objective may lead to worse SDD results than only $SObj4$, such as $SObj4$ plus $SObj1$. Therefore, the weight in multi-objective optimization should be properly selected for an accurate SDD result.

As the multi-objective function shown in Eq. 5, the weight value w ranges from 0 to 1 to generate different solutions. Therefore, the w varying from 0 to 1.0 at a regular interval of 0.1 is considered. Specially, the multi-objective function reduces to single-objective function when w equals to 0 and $SObj4$ when w equals to 1. N_M = 5 and the 100 times of calculation are used to determine DVC100. The DVC100 values of SDD results in case 3 based on varying w are listed in Table 2. Obviously, the combination of $SObj4$ is able to improve the performance of the other five single-objective functions as DVC100 values at the column of w = 0 in Table 2 are significantly smaller than those at the other columns. However, the increasing weight of $SObj4$ does not always increase SDD accuracy but sometimes leads to a decline in DVC100 values such as the combination with $SObj2$. Meanwhile, the combination of $SObj4$ and $SObj3$ shows superiority over the other four multi-objective functions. Its DVC100 value increases when the weight value is smaller than 0.1 and then gradually decline. Hence, the combination of $SObj4$ and $SObj3$ with w equaling to 0.1 provides the best solution for SDD and the conclusion will be further verified in the following two numerical simulations. The mean values of SDD results in case 3 based on the best solution are shown in Figure 5. The figure shows that the identified results without noise are highly accurate, which means the best solution effectively shows the actual structural damages.

As the SDD results based on $SObj1$ come second as shown in the above section, the combination of $SObj1$ with the other five objectives is also investigated using case 3. DVC100 values of the SDD results in case 3 are listed in Table 3. The results show that the combination of $SObj1$ and $SObj5$ provides the highest DVC100 values, whether N_M = 3 or N_M = 5. It means the solution from $SObj1$ plus $SObj5$ can be seen as the best optimal for multi-objective identification. Furthermore, the best weight for $SObj1$ is also investigated, and the results are listed in Table 4. From the table, the combination of $SObj1$ and

TABLE 4 DVC100 values of SDD results in case 3 based on varying *w*.

$J_1(\boldsymbol{\alpha})$	$J_2(\boldsymbol{\alpha})$	N_M	*w*								
			0.1	0.2	0.3	0.4	0.5	0.6	0.7	0.8	0.9
*SObj*1	*SObj*5	3	93%	80%	72%	83%	87%	71%	58%	39%	20%
*SObj*1	*SObj*5	5	100%	99%	100%	98%	96%	96%	87%	70%	59%

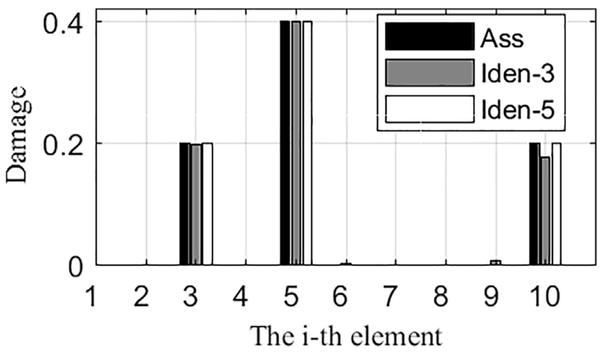

FIGURE 6
Mean values of SDD results in case 3 based on (0.1**SObj*1 + 0.9**SObj*5)

*SObj*5 with $w = 0.1$ and $N_M = 5$ has the highest value of DVC100, and the corresponding solution can be regarded as the best one for multi-objective identification, and accurate SDD results can be therefore gained.

The mean values of SDD result in case 3 based on (0.1**SObj*1 + 0.9**SObj*5) are shown in Figure 6, in which Ass, Iden-3 and Iden-5 mean assumed damage factor vector, identified results based on $N_M = 3$ and $N_M = 5$, respectively. The identified damages are almost equaled to assumed ones with a slight error, whether $N_M = 3$ or $N_M = 5$.

From the above discussion, it can be found that the weight value equaling to 0.1 both in $LWS_1(\boldsymbol{\alpha}) = w^*SObj4(\boldsymbol{\alpha}) + (1-w)^*SObj3(\boldsymbol{\alpha})$ and $LWS_2(\boldsymbol{\alpha}) = w^*SObj1(\boldsymbol{\alpha})+(1-w)^*SObj5(\boldsymbol{\alpha})$ can provide the best solution for the multi-objective identification problem.

Influences of measurement noises

In order to study the anti-noise performance of the proposed method, noise is added into frequencies and mode shapes as well. The formulation of noise contaminated in measured modal parameters is formulated as follows,

$$r_n = r_{cal}\left(1 + E_p N_{oise}\right) \tag{14}$$

where, r_n and r_{cal} are modal parameters with and without noise, respectively. E_p is the noise level. N_{oise} is a standard normal distribution vector with zero mean value and unit standard deviation. Case 3 is investigated with noise levels 1 and 2%. The first five modes are considered here, and $LWS_1(\boldsymbol{\alpha})$ and $LWS_2(\boldsymbol{\alpha})$ are both utilized with a weight equaling 0.1. The SDD results of case 3 with noise level 1 and 2% are shown in Figure 7. From the figures, the identified extent of damage shows good accuracy both by $LWS_1(\boldsymbol{\alpha})$ and $LWS_2(\boldsymbol{\alpha})$. When the noise level is 1%, the values of DVC100 of identified results based on $LWS_1(\boldsymbol{\alpha})$ and $LWS_2(\boldsymbol{\alpha})$ are 95 and 99%, respectively, which shows not only the accuracy of the SDD results but also the high stability among repeated calculations. However, the DVC100 slightly decrease when the noise level increase to 2%, and their values are 73 and 90%, respectively. However, it can be observed that the noise contamination in modal responses leads to a decline in accuracy because errors occur in the damaged elements, and misjudgments also happen to the undamaged elements such as elements 8 and 9. The reason is

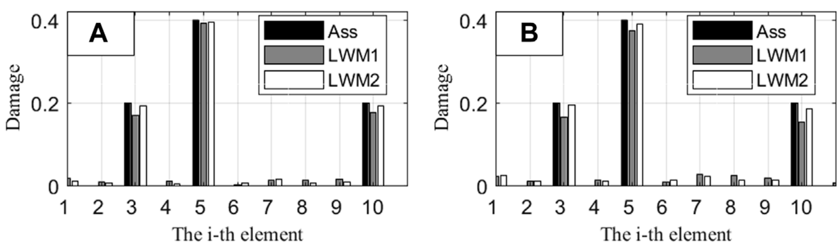

FIGURE 7
SSDD results in case 3 with noise contamination **(A)** Noise level 1%. **(B)** Noise level 2%.

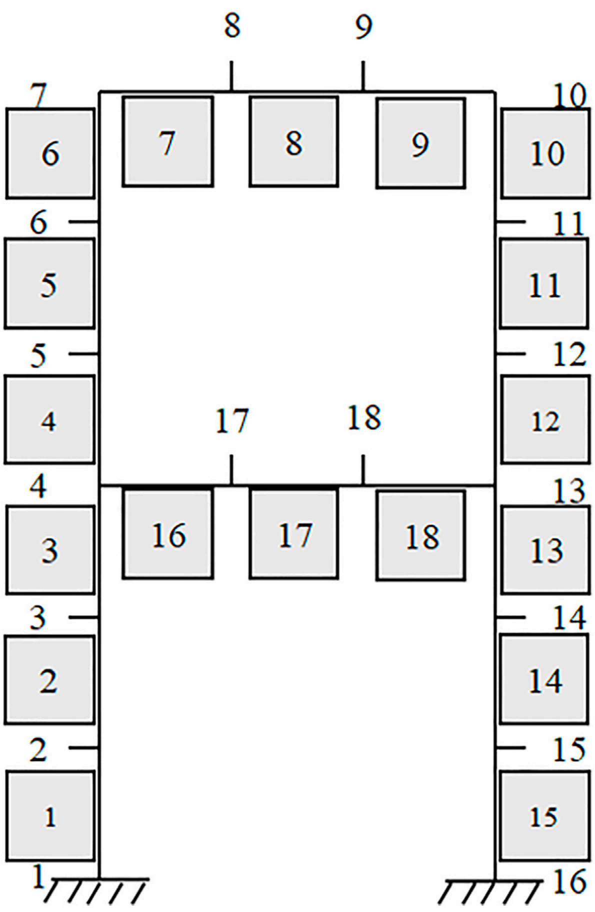

FIGURE 8
Finite element model of two-storey rigid frame structure.

that the noise contaminated in modal parameters would lead to a slight shift of the optimal point of the objectives.

SDD of two-dimensional structures

A two-storey plane steel frame

A two-storey rigid frame structure is adopted to assess the performance of the proposed method in this section. The diagram of the structure is shown in Figure 8. The elastic modulus and density of both beam and column are equal to 2.1×10^{11} N/m^3 and 7850 kg/m^3, respectively. The geometric parameters of the column are $I = 1.26 \times 10^{-5}$ m^4 and $A = 2.98 \times 10^{-3}$ m^2. And those of the beam are $I = 2.36 \times 10^{-5}$ m^4 and $A = 3.20 \times 10^{-3}$ m^2. The numbers in the box represent finite element numbers, while others denote node numbers.

The frame structure is modeled by 18 two-dimension beam elements with an equal length of 0.47 m. Four assumed cases are shown as, case 1: 20%@8; case 2: 20%@15; case 3: 20%@8, 20%@17; case 4: 40%@8, 20%@15, 20%@17; The mode shape is measured along the vertical direction of components; accordingly, the vertical direction of the beam and the horizontal direction of the column are available. The multi-objective functions $LWS_1(\boldsymbol{\alpha})$ and $LWS_2(\boldsymbol{\alpha})$ are both applied to solve the SDD problems. The first five modes are considered in this numerical simulation.

The DVC100 values of SDD results based on $LWS_1(\boldsymbol{\alpha})$ and $LWS_2(\boldsymbol{\alpha})$ with $w = 0.1$ are shown in Table 5. It can be seen that the two objectives can both accurately identify the damage in single damage cases because their DVC100 values are relatively high. However, the increase of damage element leads to a decrease in DVC100 values. Furthermore, the $LWS_2(\boldsymbol{\alpha})$ shows a better performance in dealing with multiple damage cases as its DVC100 value is higher than that of $LWS_1(\boldsymbol{\alpha})$ in cases 3 and 4.

Moreover, the mean values of all 100 times of calculations for different damage cases are determined, and they are plotted in Figure 9. It shows that the SDD results of all four damage cases are closely equaled to their assumed damage factor vectors. Although there are some misidentifications in undamaged elements such as elements 13 and 14 in case 2, their values are insignificant compared with the identified value in element 15 which is the actual damaged element. Also, it can be found that SDD results based on $LWS_2(\boldsymbol{\alpha})$ are more accurate than those based on $LWS_1(\boldsymbol{\alpha})$, which means $LWS_2(\boldsymbol{\alpha})$ exhibits superiority over $LWS_1(\boldsymbol{\alpha})$ in complex structures.

A 31-bar plane steel truss

A 31-bar planar truss is used to illustrate the proposed methods' effectiveness further and is shown in Figure 10. The parameters of the truss are as follows: elastic modulus E = 210GPa, density ρ = 7850 kg/m^3, the area and the moment of the cross-section are A = 1e-4m^2 and I = 8.3333e-10 m^4, respectively. The geometrical parameters of the truss are also shown in Figure 10 in detail. There are 31 elements in the truss, each of which has four DOFs.

Damage cases are also assumed, including single and multiple damages. Four assumed cases are shown as, case 1: 20%@15; case 2: 20%@15, 20%@30; case 3: 40%@2, 20%@15, 20%@30; case 4: 20%@2, 20%@15, 40%@31; Only LWS2(α) is applied to solve the SDD problems of the truss as the comparison of $LWS_1(\boldsymbol{\alpha})$ and $LWS_2(\boldsymbol{\alpha})$ presented in the above numerical simulation shows that the $LWS_2(\boldsymbol{\alpha})$ has better performance than $LWS_1(\boldsymbol{\alpha})$ in deal with complex structure.

The effect of N_M = 7, N_M = 15 and N_M = 20 on SDD accuracy is investigated, and the DVC100 values of SDD results are listed in Table 6. From the table, it can be found that only the DVC100 of case 1 keeps high values compared with the other three cases. It means that the

TABLE 5 DVC100 values of SDD results based on LWS_1 (α) and LWS_2 (α) with w = 0.1.

Multi-objective optimization	N_M	Case			
		1	2	3	4
$LWS_1(\boldsymbol{\alpha})$	5	85%	62%	52%	31%
$LWS_2(\boldsymbol{\alpha})$	5	84%	74%	58%	43%

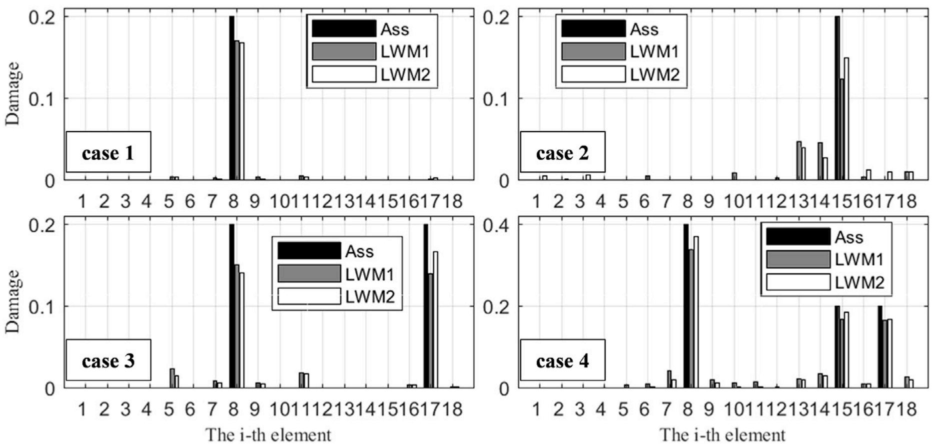

FIGURE 9
SDD results of the two-storey plane steel frame.

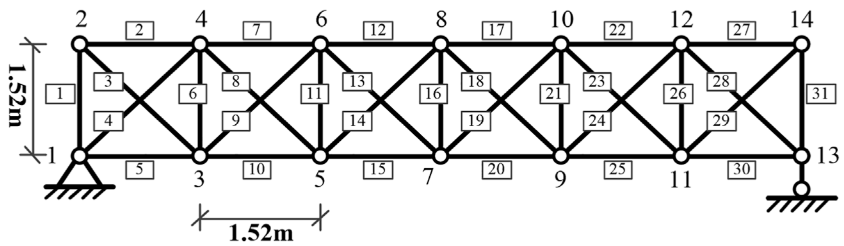

FIGURE 10
Finite element model of 31-bar planar steel truss.

TABLE 6 DVC100 values of SDD results based on LWS_2 (α) with w = 0.1.

Multi-objective optimization	N_M	Case			
		1	2	3	4
$LWS_2(\boldsymbol{\alpha})$	7	59%	20%	7%	5%
	15	75%	31%	21%	20%
	20	49%	19%	5%	4%

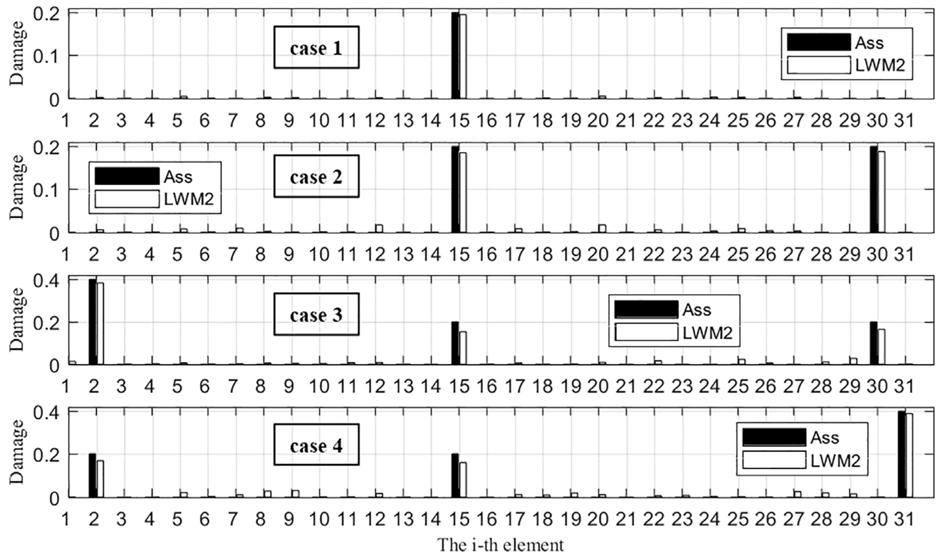

FIGURE 11
SDD results of the plane steel truss.

increase of elements would lead to more difficulty in accurate SDD. However, the SDD results considering the first fifteen modes are the most accurate, and some identification results are plotted in Figure 11. Although errors in the damaged elements and misjudgments in the undamaged elements can still be observed in the figures, their values are small. Therefore, the SDD results can satisfy the application requirement and provide effective information for structural repair.

Conclusion

In this paper, a multi-objective optimization method based on modal feature extraction and linear weight sum is proposed, and the effectiveness of the method is verified by three different kinds of structures, including a simply-supported beam, a two-story steel frame, and a 31-bar plane truss. The hybrid particle swarm optimization (HPSO) is selected as a solver to update the damage vector factor. In order to find out the best single objectives based on modal feature extraction, six single objective functions are selected, and an index named damage vector consistency (DVC) is also defined for a quantificational comparison. Moreover, the proposed multi-objective identification method based on a linear sum method also shows excellent capability in SDD. Some conclusions can be summarized as follows.

1) The *SObj*4 based on MTMAC is verified to be the best single objective function in SDD compared with the other five selected objectives. The SDD results based on *SObj*4 keep the highest possibility of capturing an accurate solution. It means that the *SObj*4 can be effectively applied to SDD problems and provide accurate SDD results.
2) The defined DVC is an effective index that quantifies the method's accuracy in a single calculation. DVC100 is the percentage of DVC values equaling 100%. It is useful to quantificationally assess the accuracy of the SDD method once more than one calculation is conducted for a damage case.
3) The proposed multi-objective identification method based on the linear sum method has good performance in SDD. The investigation shows that $LWS_1(\boldsymbol{\alpha}) = w^*SObj4(\boldsymbol{\alpha}) + (1\text{-}w)^*SObj3(\boldsymbol{\alpha})$ and $LWS_2(\boldsymbol{\alpha}) = w^*SObj1(\boldsymbol{\alpha})+(1\text{-}w)^*SObj5(\boldsymbol{\alpha})$ can both improve the SDD accuracy in different structures with various damage cases. The numerical simulations further show that the best solution can be gained from candidate solutions when $w = 0.1$. Moreover, $LWS_2(\boldsymbol{\alpha})$ performs better than $LWS_1(\boldsymbol{\alpha})$ in complex structures.

Data availability statement

The original contributions presented in the study are included in the article/Supplementary Material, further inquiries can be directed to the corresponding author.

Author contributions

ZEC: Data curation, Formal analysis, Investigation, Methodology, Software, Visualization, Writing review and editing. DZ: Formal analysis, Validation, Writing—review and editing. ZHC and WW: paper revising.

Funding

This project is supported by the National Natural Science Foundation of China with grant number 52008109, and the Open Research Fund Program of Ministry of Education Key Lab of Disaster Forecast and Control in Engineering of China with number 20200904004.

Conflict of interest

The authors declare that the research was conducted in the absence of any commercial or financial relationships that could be construed as a potential conflict of interest.

Publisher's note

All claims expressed in this article are solely those of the authors and do not necessarily represent those of their affiliated organizations, or those of the publisher, the editors and the reviewers. Any product that may be evaluated in this article, or claim that may be made by its manufacturer, is not guaranteed or endorsed by the publisher.

References

Baghmisheh, M. T. V., Peimani, M., Sadeghi, M. H., Ettefagh, M. M., and Tabrizi, A. F. (2012). A hybrid particle swarm–Nelder–Mead optimization method for crack detection in cantilever beams. *Appl. Soft Comput.* 12, 2217–2226. doi:10.1016/j.asoc.2012.03.030

Beck, J. L., and Au, S.-K. (2002). Bayesian updating of structural models and reliability using Markov chain Monte Carlo simulation. *J. Eng. Mech.* 128, 380–391. doi:10.1061/(asce)0733-9399(2002)128:4(380)

Beck, J. L., Au, S.-K., and Vanik, M. W. (2001). Monitoring structural health using a probabilistic measure. *Comp-aided. Civ. Eng.* 16, 1–11. doi:10.1111/0885-9507.00209

Behmanesh, I., Moaveni, B., Lombaert, G., and Papadimitriou, C. (2015). Hierarchical Bayesian model updating for structural identification. *Mech. Syst. Signal Process.* 64 (65), 360–376. doi:10.1016/j.ymssp.2015.03.026

Boe, P., and Golinval, J.-C. (2003). Principal component analysis of a piezosensor array for damage localization. *Struct. Health Monit.* 2, 137–144. doi:10.1177/1475921703002002005

Cawley, P., and Adams, R. D. (1979). The location of defects in structures from measurements of natural frequencies. *J. Strain Analysis Eng. Des.* 14, 49–57. doi:10.1243/03093247V142049

Cha, Y.-J., and Buyukozturk, O. (2015). Structural damage detection using modal strain energy and hybrid multiobjective optimization: Damage detection using multiobjective optimization. *Computer-Aided Civ. Infrastructure Eng.* 30, 347–358. doi:10.1111/mice.12122

Chen, C., Pan, C., Chen, Z., and Yu, L. (2019). Structural damage detection via combining weighted strategy with trace Lasso. *Adv. Struct. Eng.* 22, 597–612. doi:10.1177/1369433218795310

Chen, H.-P. (2008). Application of regularization methods to damage detection in large scale plane frame structures using incomplete noisy modal data. *Eng. Struct.* 30, 3219–3227. doi:10.1016/j.engstruct.2008.04.038

Chen, Z., and Yu, L. (2018). A new structural damage detection strategy of hybrid PSO with Monte Carlo simulations and experimental verifications. *Measurement* 122, 658–669. doi:10.1016/j.measurement.2018.01.068

Cheung, S. H., and Beck, J. L. (2009). Bayesian model updating using hybrid Monte Carlo simulation with application to structural dynamic models with many uncertain parameters. *J. Eng. Mech.* 135, 243–255. doi:10.1061/(asce)0733-9399(2009)135:4(243)

Ching, J., and Chen, Y.-C. (2007). Transitional Markov chain Monte Carlo method for bayesian model updating, model class selection, and model averaging. *J. Eng. Mech.* 133, 816–832. doi:10.1061/(asce)0733-9399(2007)133:7(816)

Chu-Dong, P., Ling, Y., Ze-Peng, C., Wen-Feng, L., and Huan-Lin, L. (2016). A hybrid self-adaptive Firefly-Nelder-Mead algorithm for structural damage detection. *Smart Struct. Syst.* 17, 957–980. doi:10.12989/SSS.2016.17.6.957

Ding, Z., Hou, R., and Xia, Y. (2022). Structural damage identification considering uncertainties based on a Jaya algorithm with a local pattern search strategy and L0.5 sparse regularization. *Eng. Struct.* 261, 114312. doi:10.1016/j.engstruct.2022.114312

Ding, Z., Li, J., Hao, H., and Lu, Z.-R. (2019a). Nonlinear hysteretic parameter identification using an improved tree-seed algorithm. *Swarm Evol. Comput.* 46, 69–83. doi:10.1016/j.swevo.2019.02.005

Ding, Z., Li, J., Hao, H., and Lu, Z.-R. (2019b). Structural damage identification with uncertain modelling error and measurement noise by clustering based tree seeds algorithm. *Eng. Struct.* 185, 301–314. doi:10.1016/j.engstruct.2019.01.118

Ding, Z., Yao, R., Li, J., and Lu, Z. (2018). Structural damage identification based on modified Artificial Bee Colony algorithm using modal data. *Inverse Problems Sci. Eng.* 26, 422–442. doi:10.1080/17415977.2017.1310855

Gao, Y., and Spencer, B. F. (2002). Damage localization under ambient vibration using changes in flexibility. *Earthq. Engin. Engin. Vib.* 1, 136–144. doi:10.1007/s11803-002-0017-x

He, M., Liang, P., Wang, Y., Xia, Z., and Wu, X. (2022). Online automatic monitoring of abnormal vibration of stay cables based on acceleration data from structural health monitoring. *Measurement* 195, 111102. doi:10.1016/j.measurement.2022.111102

He, R.-S., and Hwang, S.-F. (2006). Damage detection by an adaptive real-parameter simulated annealing genetic algorithm. *Comput. Struct.* 84, 2231–2243. doi:10.1016/j.compstruc.2006.08.031

Hou, R., and Xia, Y. (2021). Review on the new development of vibration-based damage identification for civil engineering structures: 2010–2019. *J. Sound Vib.* 491, 115741. doi:10.1016/j.jsv.2020.115741

Hou, R., Xia, Y., Zhou, X., and Huang, Y. (2019). Sparse Bayesian learning for structural damage detection using expectation–maximization technique. *Struct. Control Health Monit.* 26, e2343. doi:10.1002/stc.2343

Hou, R., Xia, Y., and Zhou, X. (2018). Structural damage detection based on l1 regularization using natural frequencies and mode shapes. *Struct. Control Health Monit.* 25, e2107. doi:10.1002/stc.2107

Hou, Z., Noori, M., and Amand, R. St. (2000). Wavelet-based approach for structural damage detection. *J. Eng. Mech.* 126, 677–683. doi:10.1061/(asce)0733-9399(2000)126:7(677)

Huang, Y., Beck, J. L., Wu, S., and Li, H. (2014). Robust bayesian compressive sensing for signals in structural health monitoring: Robust BCS in SHM. *Computer-Aided Civ. Infrastructure Eng.* 29, 160–179. doi:10.1111/mice.12051

Jaishi, B., and Ren, W.-X. (2006). Damage detection by finite element model updating using modal flexibility residual. *J. Sound Vib.* 290, 369–387. doi:10.1016/j.jsv.2005.04.006

Jung, S., Ok, S.-Y., and Song, J. (2010). Robust structural damage identification based on multi-objective optimization. *Int. J. Numer. Methods Eng.* 81, 786–804. doi:10.1002/nme.2726

Kennedy', J., and Eberhart, R. (1995). in *Particle swarm optimization*. Editor Aust Perth (New Jersey, United States: IEEE), 1942–1948.

Law, S. S., Li, X. Y., Zhu, X. Q., and Chan, S. L. (2005). Structural damage detection from wavelet packet sensitivity. *Eng. Struct.* 27, 1339–1348. doi:10.1016/j.engstruct.2005.03.014

Lieven, N. a. J., and Ewins, D. J. (1988). "Spatial correlation of mode shapes: The coordinate modal assurance criterion (COMAC)," in Proceedings of the 6th International Modal Analysis Conference (IMAC), Hyatt Orlando, Kissimmee, Florida, February 1-4 1988, 690–695.

Lin, Y., Nie, Z., and Ma, H. (2017). Structural damage detection with automatic feature-extraction through deep learning: Structural damage detection with automatic feature-extraction through deep learning. *Computer-Aided Civ. Infrastructure Eng.* 32, 1025–1046. doi:10.1111/mice.12313

Liu, B., Wang, L., Jin, Y.-H., Tang, F., and Huang, D.-X. (2005). Improved particle swarm optimization combined with chaos. *Chaos, Solit. Fractals* 25, 1261–1271. doi:10.1016/j.chaos.2004.11.095

Lu, H., Liu, L., Liu, A., Pi, Y.-L., Bradford, M. A., and Huang, Y. (2020). Effects of movement and rotation of supports on nonlinear instability of fixed shallow arches. *Thin-Walled Struct.* 155, 106909. doi:10.1016/j.tws.2020.106909

Lu, H., Zhou, J., Sahmani, S., and Safaei, B. (2021). Nonlinear stability of axially compressed couple stress-based composite micropanels reinforced with random checkerboard nanofillers. *Phys. Scr.* 96, 125703. doi:10.1088/1402-4896/ac1d7f

Lu, Z. R., Lin, X. X., Chen, Y. M., and Huang, M. (2017). Hybrid sensitivity matrix for damage identification in axially functionally graded beams. *Appl. Math. Model.* 41, 604–617. doi:10.1016/j.apm.2016.09.008

Messina, A., Williams, E. J., and Contursi, T. (1998). Structural damage detection by a sensitivity and statistical-based method. *J. Sound Vib.* 216, 791–808. doi:10.1006/jsvi.1998.1728

Miguel, F. L. F., Miguel, F. L. F., and Thomas, K. C. A. (2009). Theoretical and experimental modal analysis of a cantilever steel beam with a tip mass. *Proc. Institution Mech. Eng. Part C J. Mech. Eng. Sci.* 223, 1535–1541. doi:10.1243/09544062JMES1390

Minh, H.-L., Sang-To, T., Abdel Wahab, M., and Cuong-Le, T. (2022). Structural damage identification in thin-shell structures using a new technique combining finite element model updating and improved Cuckoo search algorithm. *Adv. Eng. Softw.* 173, 103206. doi:10.1016/j.advengsoft.2022.103206

Mu, H.-Q., and Yuen, K.-V. (2017). Novel sparse bayesian learning and its application to ground motion pattern recognition. *J. Comput. Civ. Eng.* 31, 04017031. doi:10.1061/(ASCE)CP.1943-5487.0000668

Pandey, A. K., and Biswas, M. (1994). Damage detection in structures using changes in flexibility. *J. Sound Vib.* 169, 3–17. doi:10.1006/jsvi.1994.1002

Pandey, A. K., Biswas, M., and Samman, M. M. (1991). Damage detection from changes in curvature mode shapes. *J. Sound Vib.* 145, 321–332. doi:10.1016/0022-460X(91)90595-B

Perera, R., Marin, R., and Ruiz, A. (2013). Static–dynamic multi-scale structural damage identification in a multi-objective framework. *J. Sound Vib.* 332, 1484–1500. doi:10.1016/j.jsv.2012.10.033

Perera, R., and Ruiz, A. (2008). A multistage FE updating procedure for damage identification in large-scale structures based on multiobjective evolutionary optimization. *Mech. Syst. Signal Process.* 22, 970–991. doi:10.1016/j.ymssp.2007.10.004

Perera, R., Ruiz, A., and Manzano, C. (2007). An evolutionary multiobjective framework for structural damage localization and quantification. *Eng. Struct.* 29, 2540–2550. doi:10.1016/j.engstruct.2007.01.003

Perera, R., Ruiz, A., and Manzano, C. (2009). Performance assessment of multicriteria damage identification genetic algorithms. *Comput. Struct.* 87, 120–127. doi:10.1016/j.compstruc.2008.07.003

Perera, R., and Torres, R. (2006). Structural damage detection via modal data with genetic algorithms. *J. Struct. Eng.* 132, 1491–1501. doi:10.1061/(asce)0733-9445(2006)132:9(1491)

Rao, M. A., Srinivas, J., and Murthy, B. S. N. (2004). Damage detection in vibrating bodies using genetic algorithms. *Comput. Struct.* 82, 963–968. doi:10.1016/j.compstruc.2004.01.005

Seyedpoor, S. M. (2012). A two stage method for structural damage detection using a modal strain energy based index and particle swarm optimization. *Int. J. Non-Linear Mech.* 47, 1–8. doi:10.1016/j.ijnonlinmec.2011.07.011

Shi, Z. Y., Law, S. S., and Zhang, L. M. (1998). Structural damage localization from modal strain energy change. *J. Sound Vib.* 218, 825–844. doi:10.1006/jsvi.1998.1878

Wang, C., Gao, J., Li, H., Lin, C., Beck, J. L., and Huang, Y. (2022). Robust sparse Bayesian learning for broad learning with application to high-speed railway track monitoring. *Struct. Health Monit.* 14759217221104224, 147592172211042. doi:10.1177/14759217221104224

West, W. M. (1986). Illustration of the use of modal assurance criterion to detect structural changes in an Orbiter test specimen. Available at: https://ntrs.nasa.gov/citations/19870041253.

Xiong, H., Chen, L., Yuan, C., and Kong, Q. (2021). A novel piezoceramic-based sensing Technology combined with visual domain networks for timber damage quantification. *Front. Mat.* 8. doi:10.3389/fmats.2021.688594

Xu, Y. L., and Chen, J. (2004). Structural damage detection using empirical mode decomposition: Experimental investigation. *J. Eng. Mech.* 130, 1279–1288. doi:10.1061/(asce)0733-9399(2004)130:11(1279)

Yan, A.-M., Kerschen, G., Boe, P., and Golinval, J.-C. (2005). Structural damage diagnosis under varying environmental conditions -Part I: A linear analysis. *Mech. Syst. Signal Process.* 19, 847–864. doi:10.1016/j.ymssp.2004.12.002

Yang, J. N., Lei, Y., Lin, S., and Huang, N. (2004). Hilbert-huang based approach for structural damage detection. *J. Eng. Mech.* 130, 85–95. doi:10.1061/(asce)0733-9399(2004)130:1(85)

Yi, T.-H., Huang, H.-B., and Li, H.-N. (2017). Development of sensor validation methodologies for structural health monitoring: A comprehensive review. *Measurement* 109, 200–214. doi:10.1016/j.measurement.2017.05.064

Yi, T.-H., Song, G., Stiros, S. C., and Chen, B. (2015). Distributed sensor networks for health monitoring of civil infrastructures. *Shock Vib.* 2015, 1–3. doi:10.1155/2015/271912

Yu, L., and Li, C. (2014). A global artificial fish swarm algorithm for structural damage detection. *Adv. Struct. Eng.* 17, 331–346. doi:10.1260/1369-4332.17.3.331

Yu, L., and Lin, J.-C. (2017). Cloud computing-based time series analysis for structural damage detection. *J. Eng. Mech.* 143, C4015002. doi:10.1061/(ASCE)EM.1943-7889.0000982

Yu, L., and Zhu, J. H. (2017). Structural damage prognosis on truss bridges with end connector bolts. *J. Eng. Mech.* 143, B4016002. doi:10.1061/(ASCE)EM.1943-7889.0001052

Yu, L., and Zhu, J. (2015). Nonlinear damage detection using higher statistical moments of structural responses. *Struct. Eng. Mech.* 54, 221–237. doi:10.12989/SEM.2015.54.2.221

Zhang, Y., Ma, J., and Wu, X. (2022). Locating damages of space trusses by combining cross-model modal strain energy and wavelet transform. *Structures* 44, 120–134. doi:10.1016/j.istruc.2022.07.081